

Segmentation of Fat and Fascias in Canine Ultrasound Images

Oleksiy Rybakov¹, Daniel Stromer¹, Irina Mischewski² and Andreas Maier¹

¹ Pattern Recognition Lab, Friedrich-Alexander-University Erlangen-Nuremberg

² Institut für Spezielle Zoologie und Evolutionsbiologie mit Phyletischem Museum,
Friedrich-Schiller-University Jena

oleksiy.or.rybakov@fau.de

Abstract. The connective tissue between fat and muscle termed fascia has been of interest to the recent clinical and biological research. However, in the canine and human medicine, the anatomic knowledge is still limited. To analyze the superficial fascia in canine medicine, a database with around 200 ultrasound images of one dog has been created. The superficial fascia contains fat compartments and is closely connected to the surrounding structures such as the skin's dermis and the epimysium of the muscles. This work proposes a semi-automatic and fully-automatic segmentation algorithm separating the different layers of ultrasound images of canine. Both algorithms were evaluated on a set of 24 expert-labeled images achieving high accuracy scores up to 95.9%.

1 Introduction

Fascias play an important role for the stabilization of the body of humans or animals and when fascias get overstressed, pain can be encountered. In that case, a common modality used for diagnosis of the fascia is ultrasound imaging, which works in real-time, causes no radiation exposure and is portable and cost-efficient [1,2]. One drawback of ultrasound imaging is that it is highly depended on the skills of the operator. Moreover, the quality of the images can be affected by the presence of various artifacts [3,4] which might lead to edge diffusion, making clinical diagnosis and biometric measurements more challenging.

A very important task in medical image analysis is segmentation. Usually, this technique is used to locate objects and boundaries in images. Segmentation of medical ultrasound images is considered as a challenging task due to the occurring artifacts. Although there exist many segmentation approaches of ultrasound images (e. g. the method for segmentation of ultrasound images of plantar fascia proposed by Boussouar et al. [5]), the knowledge on segmentation approaches in the field of human and canine medicine is still limited. Commonly, ultrasound images of dogs contain four layers: skin, fat, fascia and muscles (cf. Fig. 1). Our work presents two approaches – a semi-automatic and a fully-automatic algorithm – separating the four layers by subsequently segmenting the fat and the fascia layer in ultrasound images of dogs. We evaluate our proposed algorithms on a database consisting of 200 ultrasound images of one dog. The database was

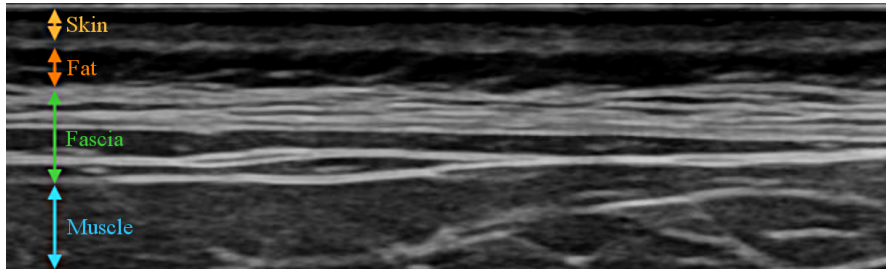


Fig. 1. An ultrasound image of a dog showing its skin, fat, fascia and muscles.

created by an expert measuring all body parts of the animal. We think that biologists working in the area of fascia research can highly benefit from our work as we will provide an open-source GUI. In addition, the resulting labeled images can be used for developing machine learning algorithms.

2 Materials and Methods

2.1 Pre-processing

Since ultrasound images tend to suffer from speckles, noise and other artifacts, we have to pre-process the input to enhance the image quality before the actual segmentation is performed. Since fascias are rather thin, it is important that the applied filters preserve edges.

The first pre-processing step is to apply Bilateral filtering. A Bilateral filter [6] is a non-linear filter commonly used in image processing to reduce noise in an image while preserving edges. The filter replaces the intensity of each pixel with a weighted average of intensity values from close pixels. Those weights $w(x, y)$ depend on the pixels' geometric and photometric distances. To reduce the runtime, we used parallel programming techniques. We also tested Guided filtering [7], however, the results for the Bilateral filter were more accurate.

In canine ultrasound images, fascias look similar to white vessels (cf. Fig. 1). In addition, fat can be also considered as a thick dark tubular structure. Frangi et al. [8] proposed an approach which achieved good results for vessel segmentation. First, the image is pre-smoothed with a Gaussian filter of scaling $s_i = (s_x, s_y)$. Then, the eigenvalues λ_1 and λ_2 of the Hessian $\mathbf{H}(x, y)$ are computed at each pixel (x, y) . Let us assume that the absolute value of the first eigenvalue λ_1 is larger than λ_2 and $\lambda_2 \approx 0$. Then, a good model for vessels is achieved if $R_B = \lambda_2/\lambda_1 \rightarrow 0$ and $S = \sqrt{\lambda_1^2 + \lambda_2^2}$ is high. Calculating

$$\mathbf{V}_{ves}(\mathbf{x}, \mathbf{y}) = \begin{cases} 0, & \text{if } \lambda_1 \approx 0 \\ \exp\left(-\frac{R_B^2}{2\beta^2}\right) \left(1 - \exp\left(-\frac{S^2}{2c^2}\right)\right), & \text{if } \lambda_1 > 0 \end{cases} \quad (1)$$

yields to a probability for the vessel where β and c denote control parameters that depend on the gray scale ($\beta = 0.5$ and $c = 4$). The calculations are performed for

different scalings s_i . The actual Vesselness is then given as the maximum over all Vesselness images for the scalings s_i . Fig. 2 shows an example ultrasound image (Left) and the output after applying the pre-processing steps (Right).

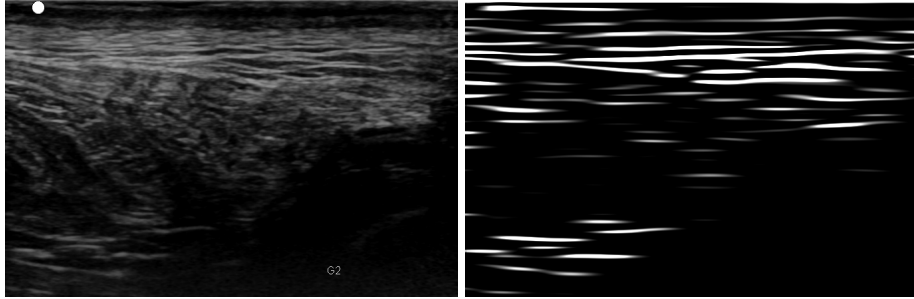


Fig. 2. (Left) Canine ultrasound image. (Right) Pre-processed image – Output after Bilateral and Vesselness filtering.

2.2 Fat Segmentation

Within the semi-automatic approach, the user can decide in which region of interest (ROI) the fat layer is located. Usually, fat can be delimited using a rectangular box aligned to the x - and y -axes of the image, where the uppermost y -coordinate does not vary from the lowermost y -coordinate by a huge number. The user sets the ROI by giving both delimiting y -coordinates as arguments.

In the automatic approach, this step is performed by a customized algorithm instead. First, for each row in the Vesselness image, we compute the amount of pixels n smaller than a certain threshold ϵ_{Fat} within the row and store those values in a histogram. For the fat layer, n tends to be high. Knowing that the fat layer is usually located in the upper part of the image, we can restrict the histogram to the upper part of our image. Then, we are searching for the minima close to the global maximum inside the restricted region. This maximum corresponds to the center of the fat layer. Since the Vesselness measure gets higher at the boundary of the fat image, a good approach to find the rows delimiting the fat layer would be to search for minima close to the global maximum. In order to prevent arriving at too high minima, high local minima are deprecated. Afterwards, the Vesselness measure at each pixel within the ROI is compared to a pre-defined threshold. If the Vesselness value at a pixel within the ROI is lower than the threshold, the pixel is classified as fat, otherwise as no-fat-area.

Since the quality of the segmentation can still be corrupted by small artifacts, several post-processing steps are applied to the segmented image. The first step in this pipeline is to remove smaller artifacts by applying morphological operators like dilation and erosion [9]. Additionally, some segmented images tend to have a top layer which does not belong to the actual fat layer. Usually, if the

most pixels of the upper boundary of the top layer are also located at the upper boundary of the rectangular box, the pixels can be classified as top-layer-pixels. The remaining parts of the top layer can be removed by applying another dilation step. Afterwards, the image might have some gaps inside the fat layer due to occlusion. Those gaps have to be removed since the fat layer has to be homogeneous. For this purpose, each column of the image is traversed and subdivided into intervals where each pixel has been classified as fat. The remaining no-fat regions in the column apart from the uppermost and the lowermost no-fat regions are then filled with the color corresponding to the fat layer. Finally, the image is smoothed by applying median filtering.

2.3 Fascia Segmentation

The semi-automatic approach for fascia segmentation is similar to our fat segmentation approach. Again, within the semi-automatic approach the user has to define a ROI where the fascia is located. Since the lower boundary of fat corresponds to the upper boundary of the fascia, only the lower boundary of the fascia has to be defined by the user. However, a rectangular box does usually not model fascias correctly. Instead, a good model to delimit the fascia is given by two intersecting straight lines (cf. Fig. 3 (Left)). The left straight line intersects the points $(0, y_l)$ and (x_c, y_c) . The right straight line intersects the points (x_c, y_c) and $(w - 1, y_r)$ where w is the width of the image. Within the semi-automatic approach, the remaining four coordinates y_l , x_c , y_c and y_r are then given to the segmentation algorithm as input parameters.

In the fully-automatic approach, this step is performed by a customized algorithm similar to the one from automatic fat segmentation. Like fascias, muscles tend to have a large Vesselness measure. However, fascias and muscles are separated by a small layer of low Vesselness measures. The boundary between fascia and muscle is then obtained by finding the rightmost local minimum within the fascia-muscle region that is small enough. Afterwards, each pixel within the resulting ROI has to be compared with the Vesselness measure at the same pixel. If, and only if, the Vesselness image at a pixel is higher than a pre-defined threshold, the pixel is classified as fascia. The resulting fascia is shown in the central image of Fig. 3. However, since fascias are usually non-homogeneous, a linear interpolation step is performed to get the complete area of the fascia. Afterwards, the image is smoothed by applying median filtering. The result is shown in Fig. 3 (Right). Finally, thresholding can be applied to the interpolated image to distinguish between fascial structures (high Vesselness measure) and fat compartments within the fascia region (low Vesselness measure).

3 Experiments and Results

The proposed algorithms have been evaluated on a database with 213 ultrasound images of one single dog, where 24 images have been manually segmented by an expert. For the remaining 189 images, the semi-automatic segmentation has been

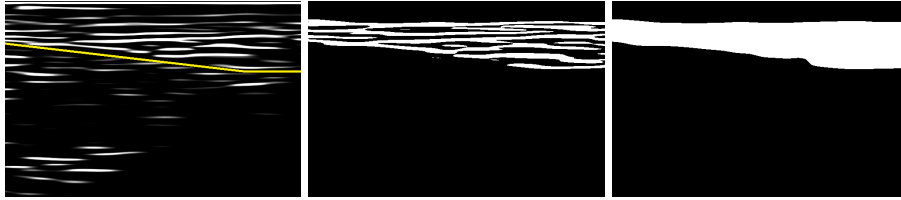


Fig. 3. (Left) A model to delimit the fascia by two straight lines (yellow). (Center) Segmented fascia structure. (Right) Interpolated area of the fascia.

Table 1. Performance measures for fully- and semi-automatic segmentation algorithm.

Measure	Accuracy	Sensitivity	Precision	Specificity	F1 score
Semi-automatic fat	98.6%	78.6%	82.6%	99.4%	80.0%
Fully-automatic fat	98.4%	79.7%	80.7%	99.2%	78.8%
Semi-automatic fascia	95.9%	92.8%	76.4%	96.0%	83.1%
Fully-automatic fascia	93.8%	74.1%	78.6%	97.6%	72.1%
Semi-automatic combined	95.9%	93.3%	83.3%	96.1%	87.8%
Fully-automatic combined	93.6%	79.6%	84.1%	97.4%	79.8%

selected as the ground truth image. The given problem can be reduced to a two-class task where positives are given by fat and fascia while negatives show the background. Table 1 shows how our two presented algorithms performed on the manually labeled dataset with respect to commonly used accuracy measures [10]. One can see, that the semi-automatic approach shows promising results with a F1 score of 80.0% for fat and 83.1% for fascia segmentation whereas the fully-automatic version has a F1 score of 78.8% for fat and 72.1% for fascia segmentation. An example of the completed segmentation is visualized in Fig. 4.

4 Discussion and Outlook

We presented a semi- and a fully-automatic segmentation algorithm for fat and fascia within ultrasound images of canines. We evaluated our developed algorithms on a expert-labeled dataset of 24 images where the F1 score of the semi-automatic approach (87.8%) is higher than the fully-automatic’s (79.8%), however, both algorithms perform well. We think that the proposed methods can be very useful for biologists as well as computer scientists. Biologists do not need to manually segment their images anymore and are able to measure fascia and fat layers efficiently. Furthermore, the newly generated labeled data can be used as a training set for future machine learning algorithms in fascia research. As the fat and fascia layers of humans do not differ a lot from canines, the algorithms can be easily extrapolated to ultrasound images of humans. The GUI will be released with the publication of the paper.

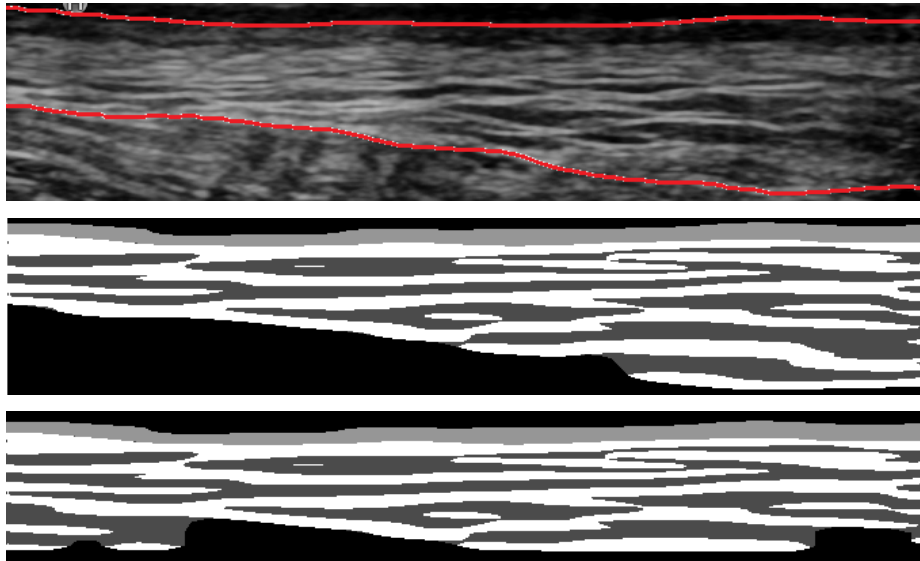


Fig. 4. (Top) Ground truth image. The fat and the fascia are delimited by the red lines. (Center) Semi-automatic resulting segmentation. (Bottom) Fully-automatic resulting segmentation. – Light Grey area denotes fat, dark gray are fat compartments within the fascia and white area denotes fascia.

References

1. Pope JA. Medical physics: imaging. Heinemann; 1999.
2. Szabo TL. Diagnostic Ultrasound Imaging: Inside Out. Academic Press Series in Biomedical Engineering. Academic Press; 2013.
3. Gonzalez RC, Woods RE, Eddins SL. Digital Image processing using MATLAB. Upper Saddle River, NJ: Prentice Hall; 2002.
4. Nelson TR, Pretorius DH, Hull A, Riccabona M, Sklansky MS, James G. Sources and impact of artifacts on clinical three-dimensional ultrasound imaging. *Ultrasound in obstetrics & gynecology*. 2000;16(4):374–383.
5. Boussouar A, Meziane F, Crofts G. Plantar fascia segmentation and thickness estimation in ultrasound images. *Computerized Medical Imaging and Graphics*. 2017;56:60–73.
6. Tomasi C, Manduchi R. Bilateral filtering for gray and color images. In: *Computer Vision, 1998. Sixth International Conference on*. IEEE; 1998. p. 839–846.
7. He K, Sun J, Tang X. Guided image filtering. *IEEE transactions on pattern analysis and machine intelligence*. 2013;35(6):1397–1409.
8. Frangi AF, Niessen WJ, Vincken KL, Viergever MA. Multiscale vessel enhancement filtering. In: *International Conference on Medical Image Computing and Computer-Assisted Intervention*. Springer; 1998. p. 130–137.
9. Heijmans HJ. Connected morphological operators for binary images. *Computer Vision and Image Understanding*. 1999;73(1):99–120.
10. Goutte C, Gaussier E. A probabilistic interpretation of precision, recall and F-score, with implication for evaluation. In: *ECIR*. vol. 5. Springer; 2005. p. 345–359.